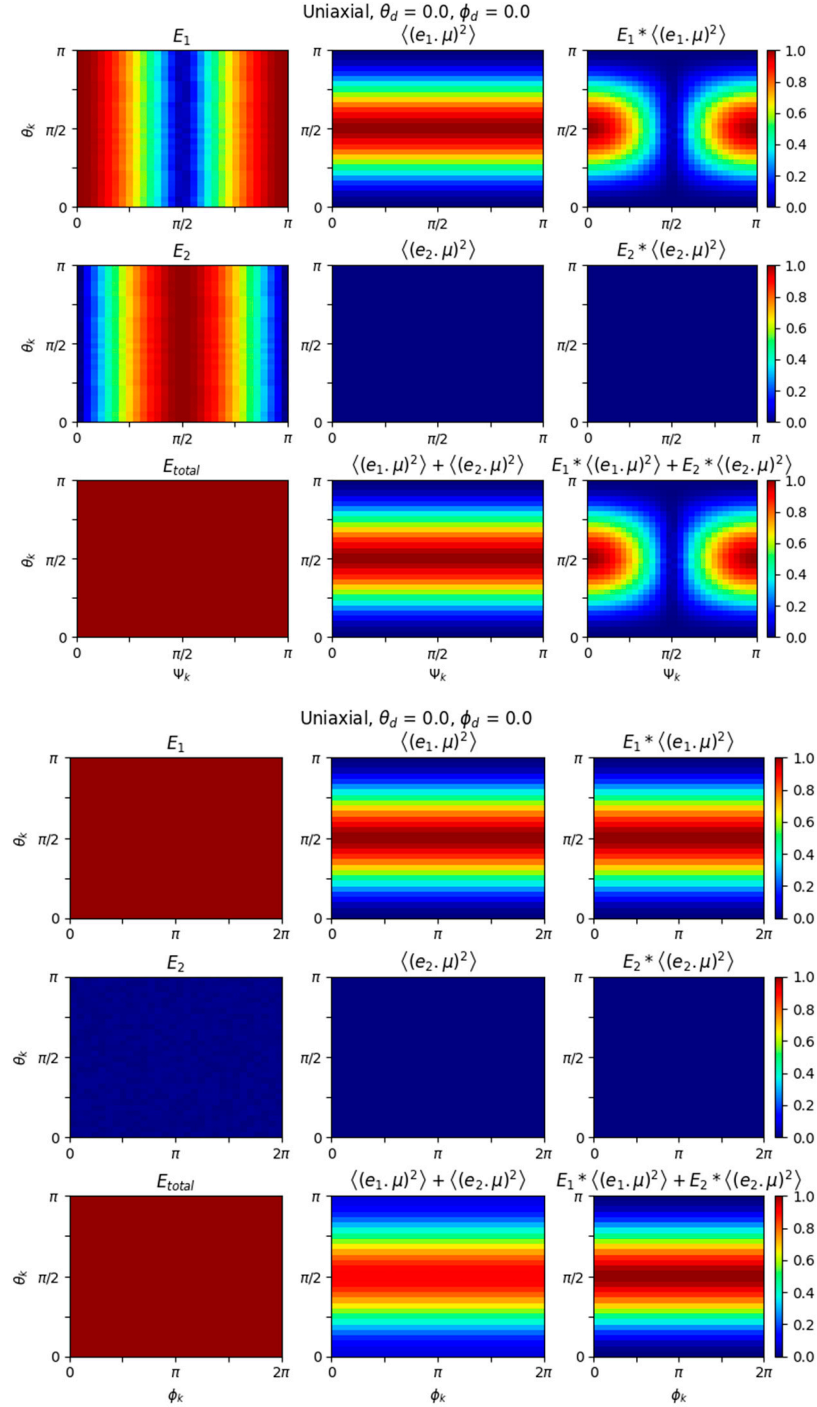


# Supplementary materials for

Linear and Non-Linear Population Retrieval with Femtosecond Optical Pumping of Molecular Crystals for the Generalised Uniaxial and Biaxial Systems

Christopher D. M. Hutchison, Alisia Fadini and Jasper J. van Thor

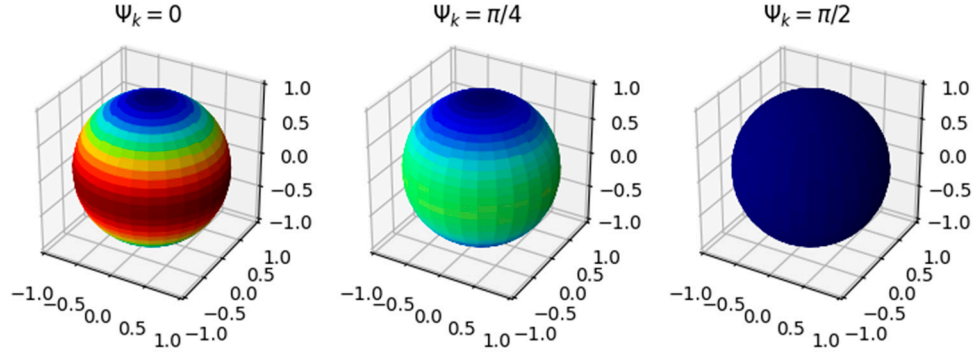
## 1. Uniaxial crystal distributions



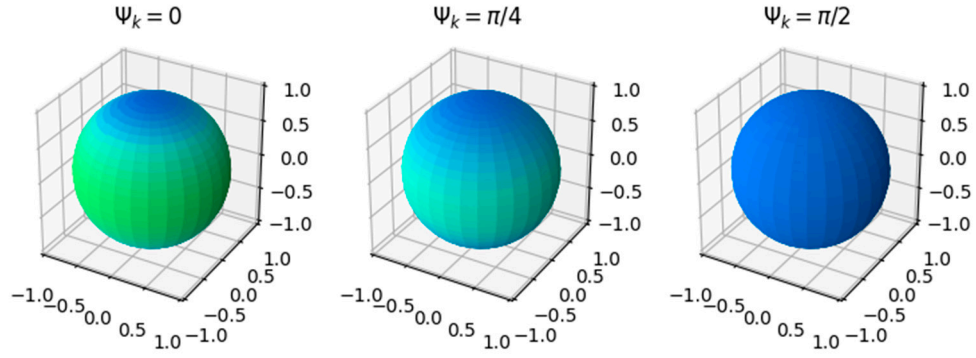
**Figure S1.** Uniaxial crystal electric field and  $E * \langle \hat{\mu} \cdot \hat{e} \rangle^2$  distributions expressed of  $\theta_k$  &  $\phi_k$  (top) and  $\theta_k$  &  $\psi_k$  for a dipole aligned with the high symmetry axis. I

can be seen that no  $\phi_k$  dependence can be seen due to the symmetry about the high symmetry axis.

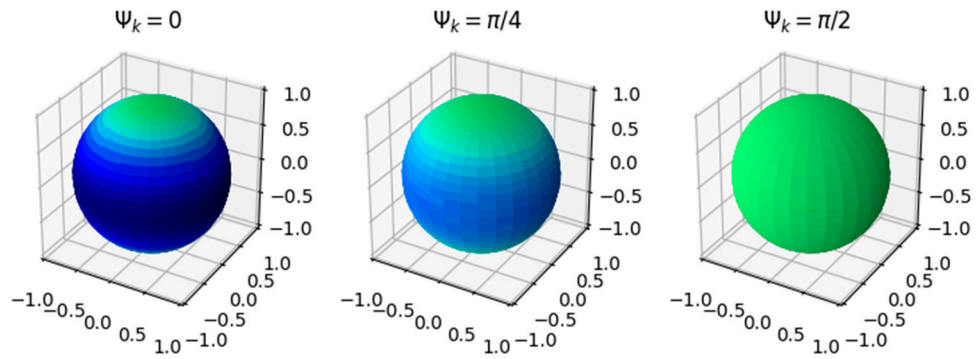
Uniaxial,  $\theta_d = 0.0$ ,  $\phi_d = 0.0$



Uniaxial,  $\theta_d = 0.785$ ,  $\phi_d = 0.0$

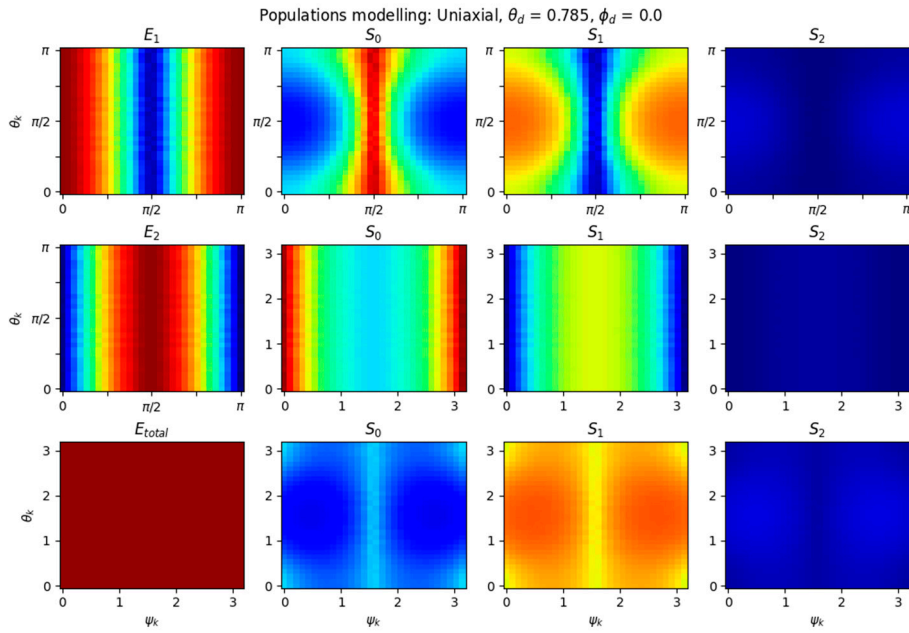
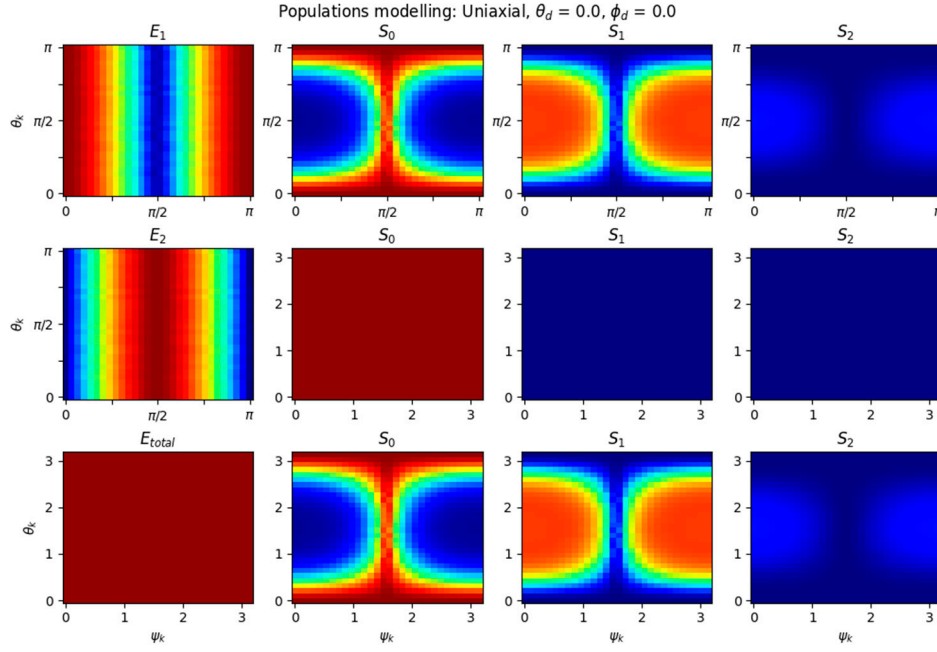


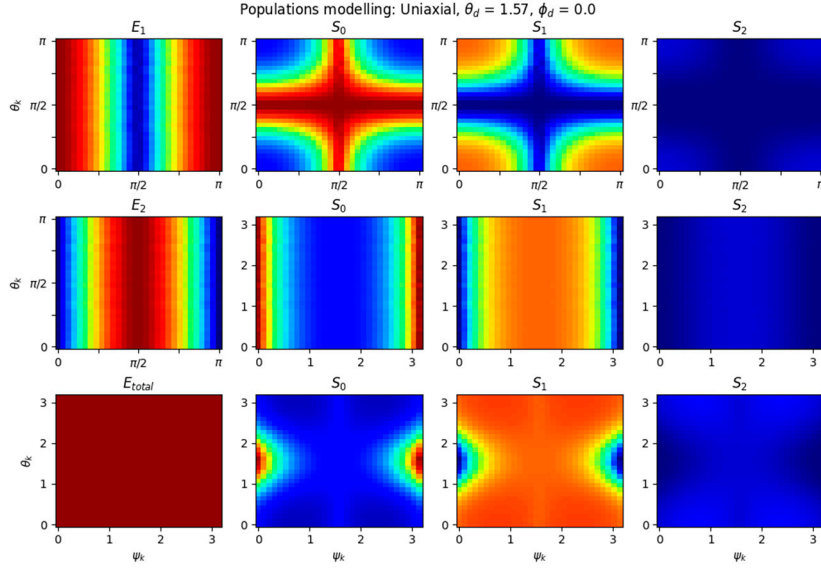
Uniaxial,  $\theta_d = 1.57$ ,  $\phi_d = 0.0$



**Figure S2.** Three-dimensional uniaxial distributions representations of the values of  $\langle E_n * (\mu \cdot e_n)^2 \rangle$  for several dipole projections.  $\theta_d = 0.0$  (top),  $\pi/4$  (middle) &  $\pi/2$

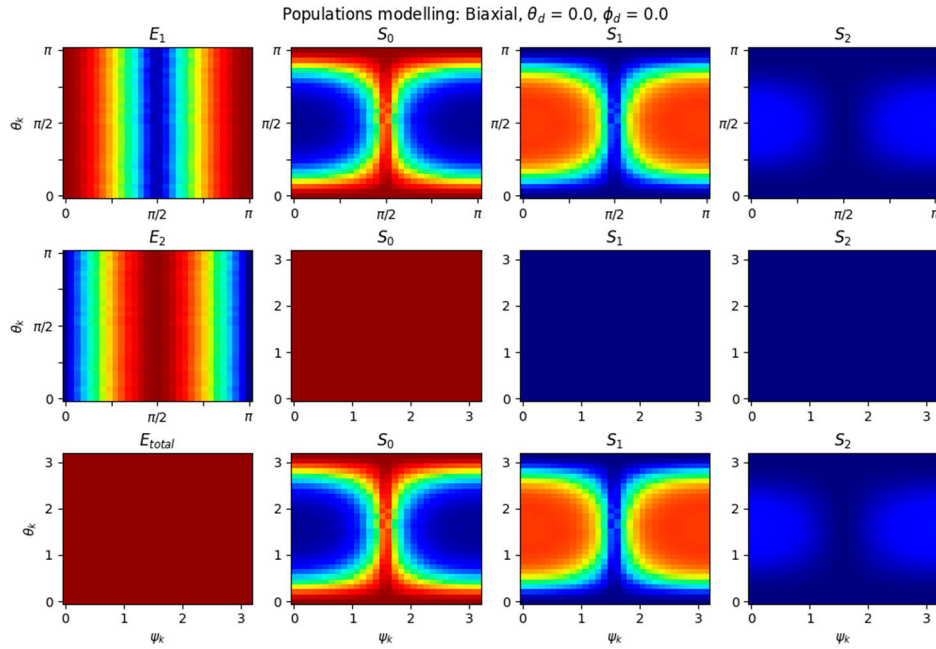
(bottom). In each case the values of  $\theta_k$  and  $\phi_k$  are polar and azimuth angles of the spheres with three different values of  $\psi_k$  displayed. It can be seen that the effect of the helical symmetry of the space group causes larger variation and maximum values when the dipole is aligned with the high symmetry axis while a more uniform but lower maximum values when aligned perpendicular to it.

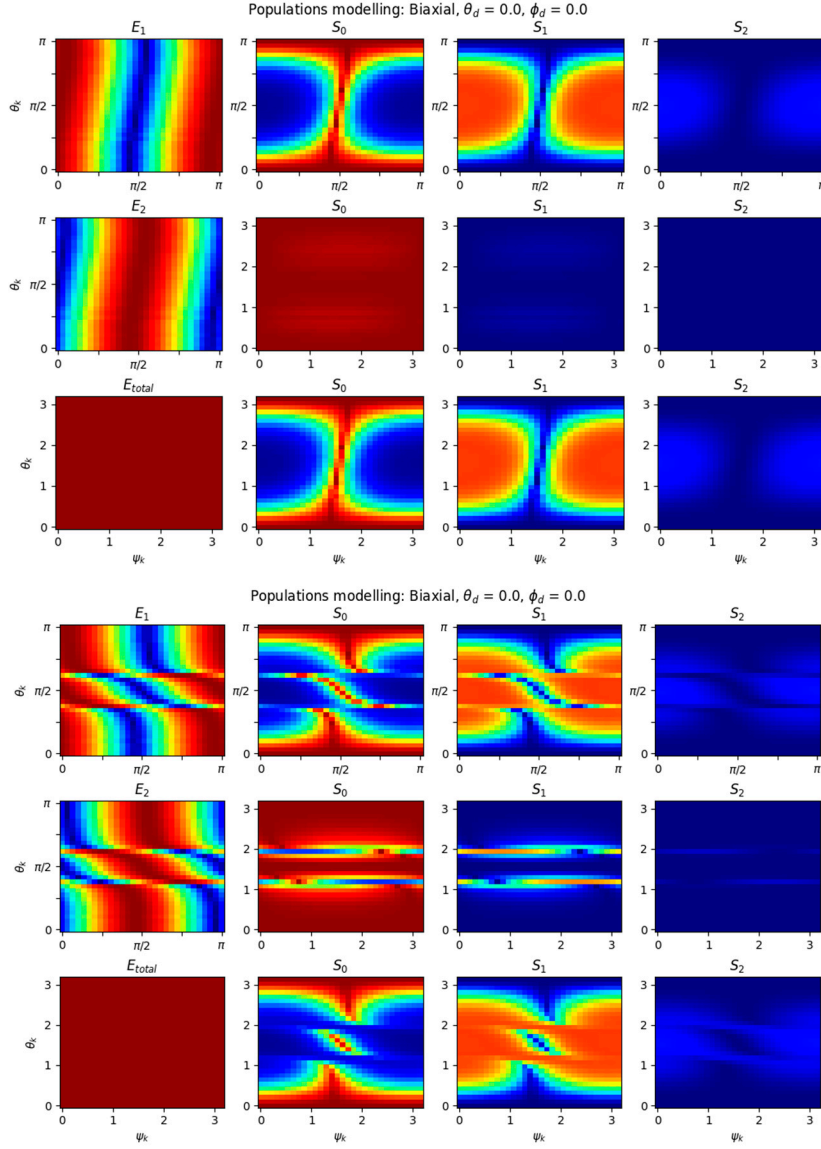




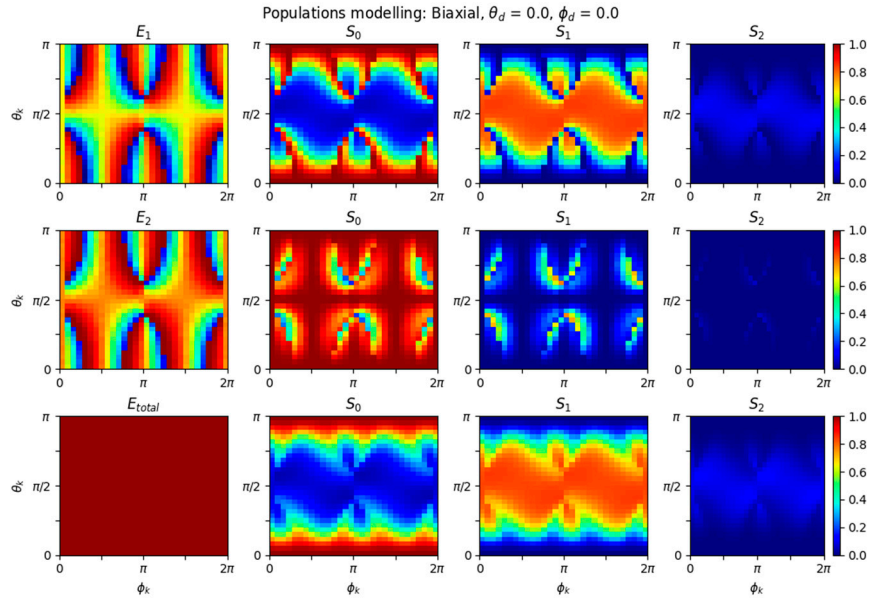
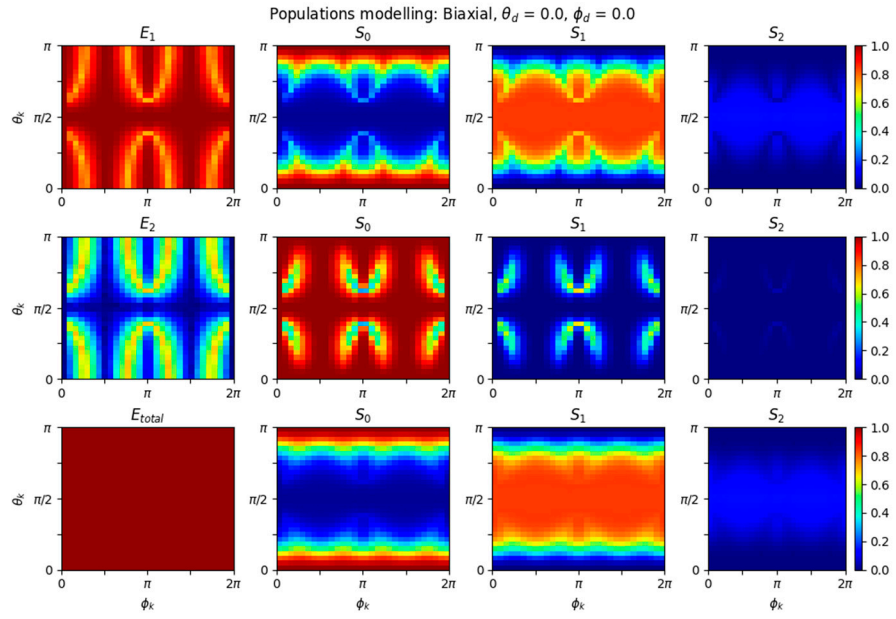
**Figure S3.** Population distributions of the uniaxial crystals with values of  $\theta_d = 0.0$  (top),  $\pi/4$  (middle) &  $\pi/2$  (bottom). In each case the pump pulse had a pulse energy of  $1 \mu\text{J}$  in a  $100 \mu\text{m}$  spot (FWHM) and a pulse length of  $130 \text{ fs}$ . The extinction coefficients used were  $\epsilon_{S0 \rightarrow S1} = 44000 \text{ M}^{-1}\text{cm}^{-1}$ ,  $\epsilon_{S1 \rightarrow S2} = 2000 \text{ M}^{-1}\text{cm}^{-1}$  &  $\epsilon_{nl} = 28000 \text{ M}^{-1}\text{cm}^{-1}$ . This reproduces Figures 5 & 6 from Hutchison et al. [12] with following correction of the factor of  $1/2$  seen in the  $\theta_d$  dependence in the ordinary directions now included which was previously omitted from the original manuscript in error.

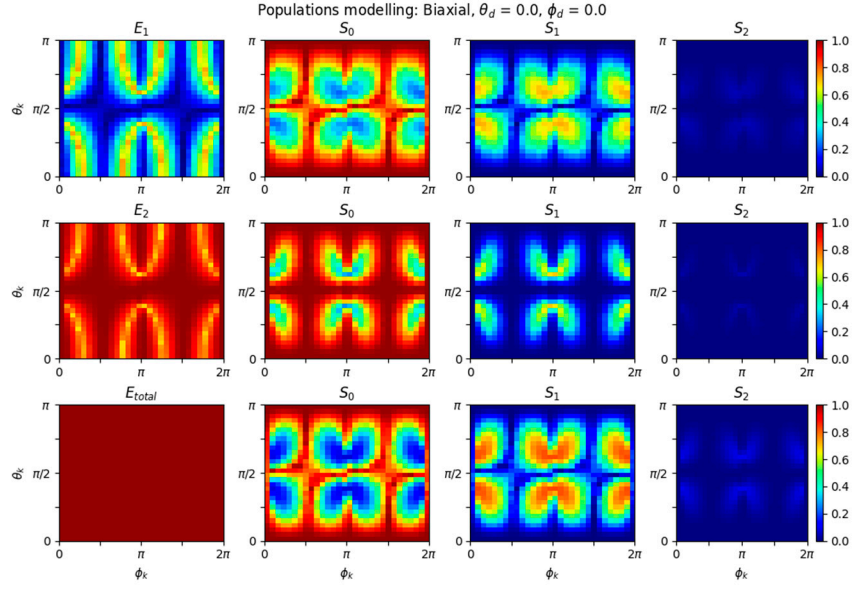
## 2. Biaxial (muscovite-like) additional population plots





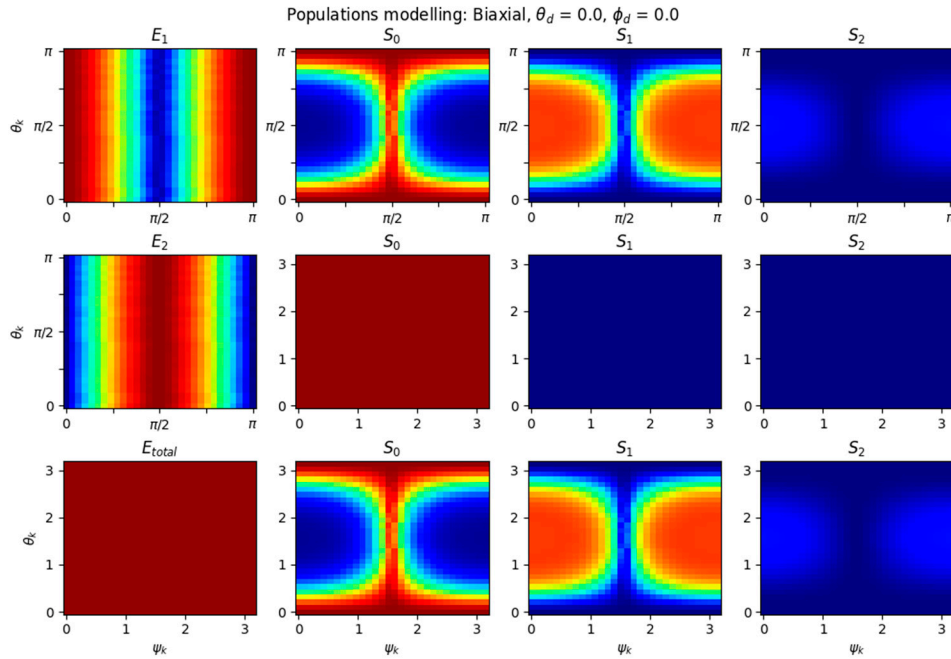
**Figure S4.** Modelled population distributions for a muscovite-like refractive index distribution plotted over  $\theta_k$  &  $\psi_k$  for values of  $\phi_k = 0$  (top)  $\phi_k = \pi/4$  (middle) and  $\phi_k = \pi/2$  (bottom). In each case the crystal was excited by a 130 fs, 1  $\mu$ J pulse in a 100  $\mu$ m (FWHM) spot. In each case the cross sections were  $\sigma_{S_0 \rightarrow S_1} = 7.3 \times 10^{-17} \text{ cm}^{-1}$   $\sigma_{S_1 \rightarrow S_2} = 3.32 \times 10^{-18} \text{ cm}^{-1}$  and  $\sigma_{S_{nl}} = 4.6 \times 10^{-17} \text{ cm}^{-1}$ .





**Figure S5.** Modelled population distributions for a muscovite-like refractive index distribution plotted over  $\theta_k$  &  $\phi_k$  for values of  $\psi_k = 0$  (top)  $\psi_k = \pi/4$  (middle) and  $\psi_k = \pi/2$  (bottom). In each case the crystal was excited by a 130 fs, 1  $\mu$ J pulse in a 100  $\mu$ m (FWHM) spot. In each case the cross sections were  $\sigma_{S_0 \rightarrow S_1} = 7.3 \times 10^{-17} \text{ cm}^{-1}$   $\sigma_{S_1 \rightarrow S_2} = 3.32 \times 10^{-18} \text{ cm}^{-1}$  and  $\sigma_{S_{nl}} = 4.6 \times 10^{-17} \text{ cm}^{-1}$ .

### 3. Biaxial (topaz-like) additional population plots



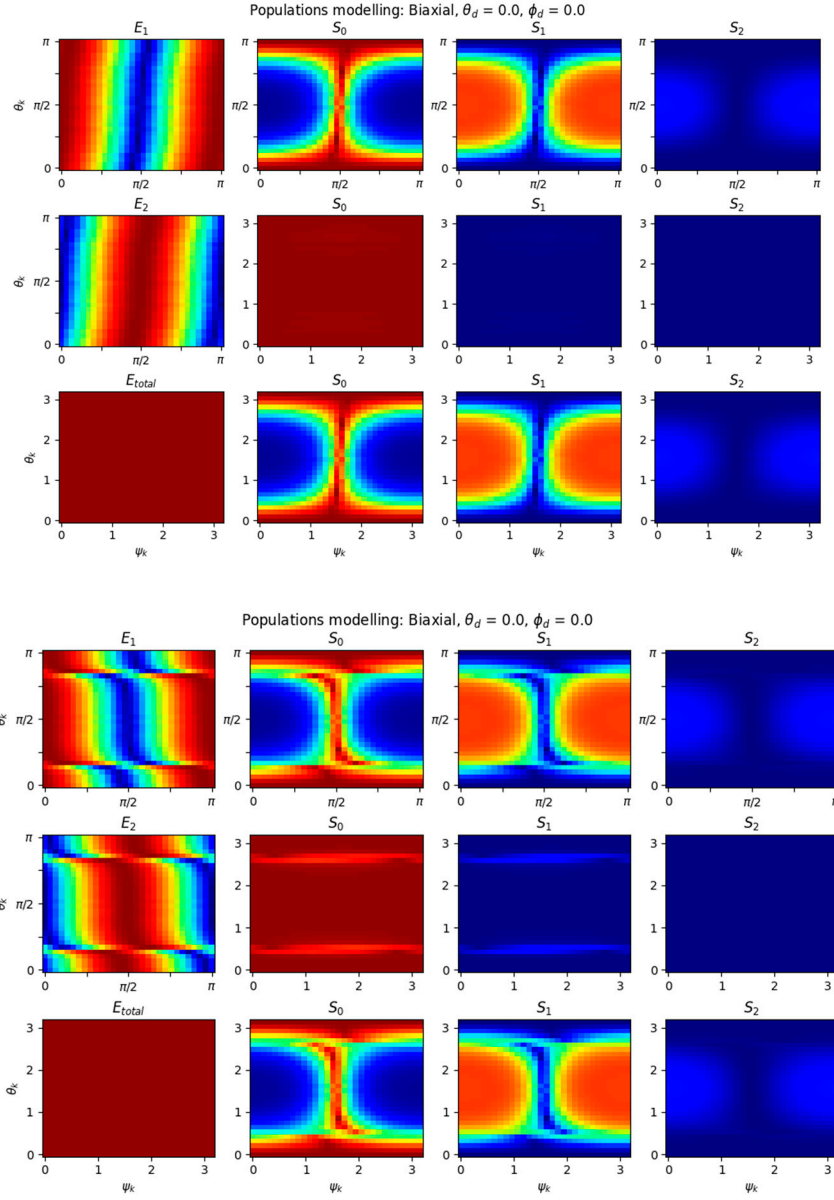


**Figure S6.** Modelled population distributions for a topaz-like refractive index distribution plotted over  $\theta_k$  &  $\psi_k$  for values of  $\phi_k = 0$  (top)  $\phi_k = \pi/4$  (middle) and  $\phi_k = \pi/2$  (bottom). In each case the crystal was excited by a 130 fs, 1  $\mu$ J pulse in a 100  $\mu$ m (FWHM) spot. In each case the cross sections were  $\sigma_{S_0 \rightarrow S_1} = 7.3 \times 10^{-17} \text{ cm}^{-1}$   $\sigma_{S_1 \rightarrow S_2} = 3.32 \times 10^{-18} \text{ cm}^{-1}$  and  $\sigma_{S_{nl}} = 4.6 \times 10^{-17} \text{ cm}^{-1}$ .

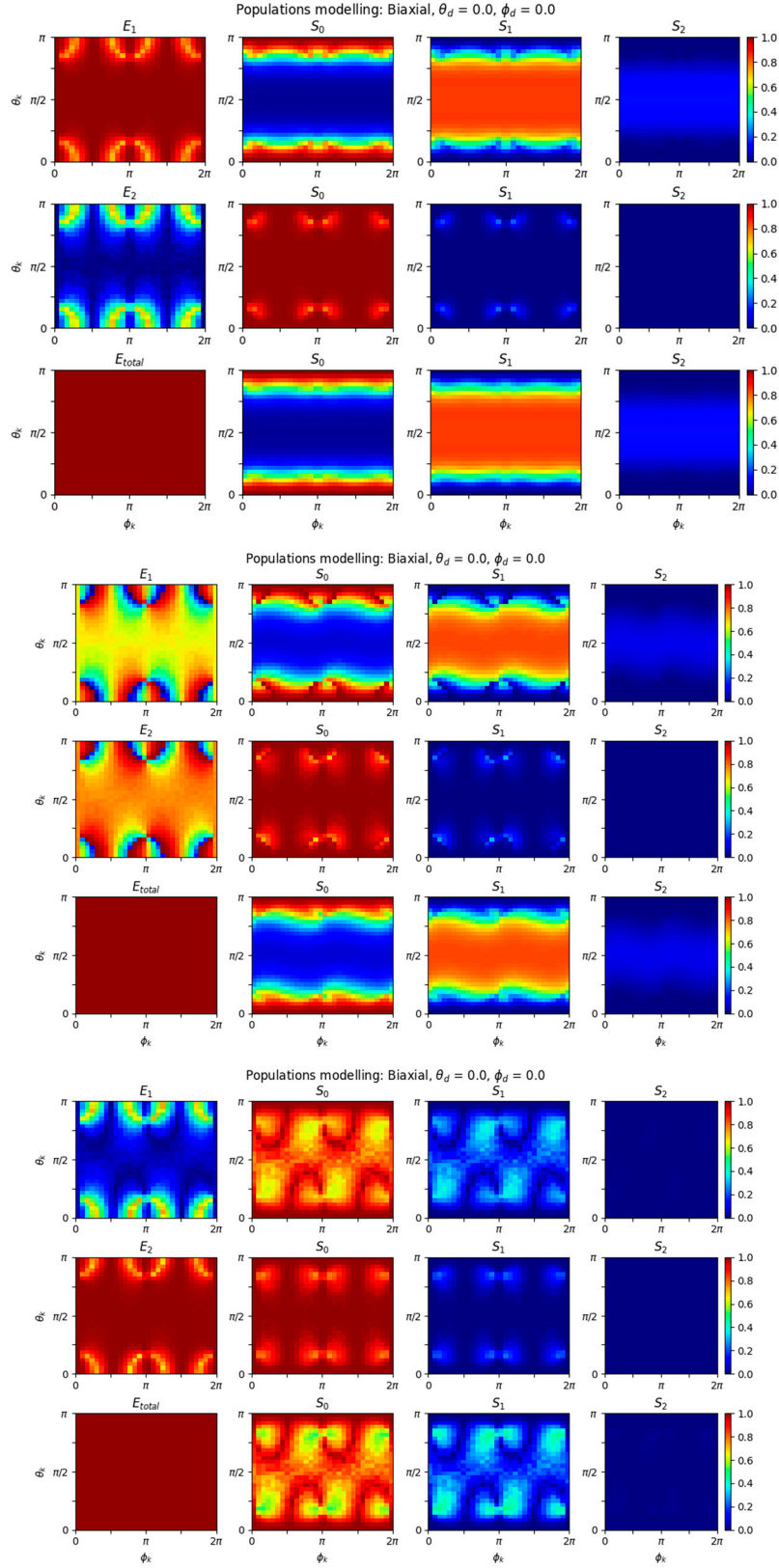


**Figure S7.** Modelled population distributions for a topas-like refractive index distribution plotted over  $\theta_k$  &  $\phi_k$  for values of  $\psi_k = 0$  (top)  $\psi_k = \pi/4$  (middle) and  $\psi_k = \pi/2$  (bottom). In each case the crystal was excited by a 130 fs, 1  $\mu$ J pulse in a 100  $\mu$ m (FWHM) spot. In each case the cross sections were  $\sigma_{S_0 \rightarrow S_1} = 7.3 \times 10^{-17} \text{ cm}^{-1}$   $\sigma_{S_1 \rightarrow S_2} = 3.32 \times 10^{-18} \text{ cm}^{-1}$  and  $\sigma_{S_{nl}} = 4.6 \times 10^{-17} \text{ cm}^{-1}$ .